

DETECTION OF THE IMPACT-GENERATED LUNAR EJECTA CLOUD BY LRO/LAMP. D. A. Glenar¹, T. J. Stubbs², C. Grava³ and K. D. Retherford⁴ ¹Univ. of Md., Baltimore Co., MD 21250, dglennar@umbc.edu, ²Code 695, NASA/GSFC, Greenbelt, MD 20771, ^{3,4}Southwest Research Institute, San Antonio, TX 78238

Introduction: During the approximately seven month duration of the LADEE mission, the Lunar Dust Experiment (LDEX) made in situ measurements of an extended but tenuous dust ejecta cloud produced by impacts from several sporadic meteoroid sources, with a peak in abundance centered near the Moon's orbital apex (dawn limb) [1]. These measurements resulted in an empirical model for the steady-state dust abundance, as a function of local solar time, altitude and power-law size distribution [2],[3]. Although the limiting sphere-equivalent grain radius for discrete detection by LDEX was $a \sim 0.3 \mu\text{m}$, the model allows for extrapolation to smaller cutoff radii ($a_{\text{min}} < 0.3 \mu\text{m}$). Such a full description of the lunar dust ejecta cloud makes it possible to model the scattering of sunlight from almost any perspective, and then use these simulations to guide a search for dust in existing (or planned) optical data sets. The use of optical remote sensing opens the possibility of long term characterization of the dust ejecta cloud, even from the lunar surface.

During 2012-2013, the Lyman Alpha Mapping Project aboard Lunar Reconnaissance Orbiter (LRO/LAMP) carried out a campaign of limb observations designed to search for dust scattering near the long wavelength end of its wavelength coverage (170-193 nm). These measurements were first analyzed in terms of an expected low altitude dust distribution [4]. Perhaps for this reason, no clear dust signature was observed and this study yielded only upper limits for dust abundance.

We have reanalyzed the LAMP dawn observations (four altogether), guided closely by simulations of the ejecta cloud radiance. Sample results, which we show below, show an unambiguous detection of light scattering by the dust exosphere.

Scattering model: Figure 1 summarizes the simulation code architecture. We utilize a library of discrete dipole (DDA) scattering properties [5], computed for multiple grain sizes, shapes and wavelengths [6]. Our present extrapolation of the model grid to large grains using Hapke slab models [7] is coarse, but sufficiently accurate at small scattering angles. Although the shape (i.e. compactness or porosity) of the dust grains is virtually unknown, the influence of shape can still be examined by overplotting the scattering from several grain shapes of

equivalent mass, ranging from sphere to loose aggregate.

This strategy is applied in Fig. 2 which shows dust spectral radiance predictions, spanning UV to near-IR wavelengths, as observed by a spacecraft in lunar shadow with sightline(s) pointed over the dawn limb [4]. We include the sensitivity limit of LAMP on this plot to illustrate that detection of the steady-state cloud with LAMP should be marginal but achievable. Despite declining solar irradiance, ultraviolet observations have distinct advantages over longer wavelengths: 1.) The scattering cross section of smaller grains increases with decreasing wavelength, and 2.) zodiacal light will not be an interfering background source, which is the case at longer wavelengths.

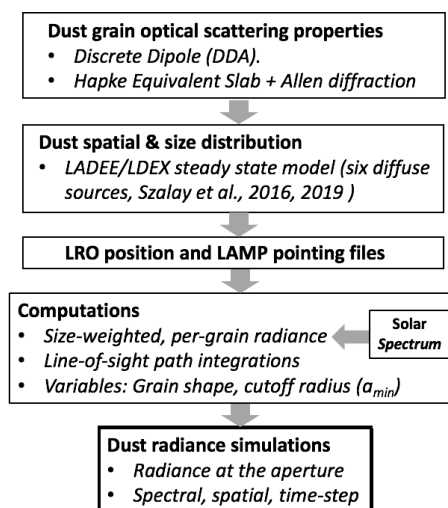


Figure 1. Simulation Code Architecture

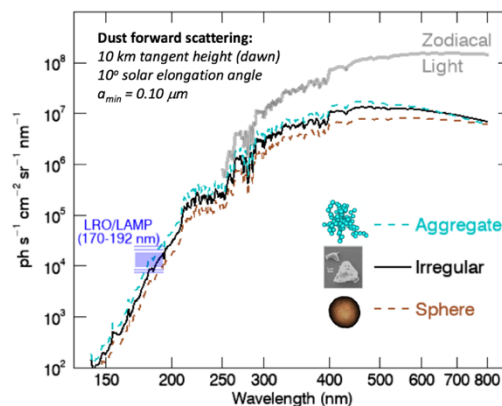


Figure 2. Predicted Cloud Spectral Radiance

LAMP Data Reduction: Because LRO is in a polar orbit, there are two windows of opportunity each year when the orbital beta angle allows dawn limb observations from lunar shadow. An observation consists of a spacecraft slew to the dawn limb and a limited duration (2-4 minute) data acquisition period with the 20 useable detector pixels of LAMP oriented perpendicular to the limb, and read at a cadence of once per second. During this time, the spacecraft travels 5-10 deg in latitude and detector pointing drifts toward or away from the Sun by 1-2 deg. Maximizing brightness change during the measurement enables the best data-model comparisons and hence the most confident detections. The resulting data cube, with dimensions $N_{\text{steps}} \times N_{\text{pixels}} \times N_{\lambda}$ is reduced via several steps:

1. Data is summed in wavelength into two spectral bands; 170-192 nm containing > 95% of the dust signal, and a 140-170 nm reference band with nearly the same intensity of instrument scattered Ly- α . Subtracting the reference map removes the Ly- α component.
2. Stars in the difference map are removed from the map histogram using a Tukey outlier rejection algorithm. These locations (and limb) are excluded from further data reduction.
3. Signal-to-noise in the result map is typically < 0.1, so the map is smoothed using a 2D moving boxcar, leaving only large scale spatial structure.

Results: The sample result map in Figure 3a, from the July 12, 2012 LAMP observation, reveals a weak dust signal. This is confirmed to be ejecta cloud scattering by comparison with the model simulation (b), computed for a population of irregular grains (see Fig. 2) and cutoff radius $a_{\text{min}}=0.1 \mu\text{m}$ in the size distribution. Contour lines indicate solar elongation angle. Dust band radiance is in units of Rayleighs (R). Panel c) compares the data and model column average radiances. In this and at least two other dawn observations, the measured dust radiance appears to be systematically higher than the models, by factors of 1.5-2 for a cutoff grain radius of $0.1 \mu\text{m}$. The measurement error bar shown in (c) represents systematic (uniform up-down) uncertainty. This is obtained from only four sky-pointing data sets, so it may underestimate the real systematic error.

Two of the dawn observations (not shown here) were made close to the galactic equator, and contaminated by dense fields of bright UV stars. In these instances, quantitative comparisons of measurement and

model are questionable, although the expected brightness trends can still be observed in the maps. These cases will be discussed.

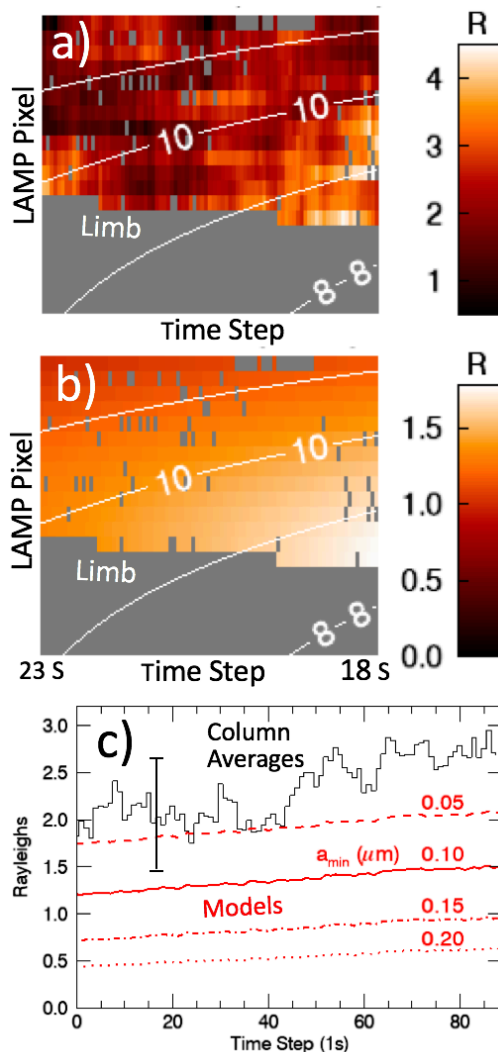


Figure 3. Sample Dust Detection

Acknowledgments: Glenar and Stubbs were supported by the NASA GSFC Internal Scientist Funding Model (ISFM). All authors were supported by LRO/LAMP.

References: [1] Horanyi M. et al. (2015) *Nature*, 522, 325. [2] Szalay J. R. and Horanyi M. (2016) *GRL*, 43, 4893-4898. [3] Szalay J. R. et al. (2019) *JGR: Planets*, 124, 143-154. [4] Feldman P. D. et al. (2014) *Icarus*, 233, 106-113. [5] Draine B. T. and Flatau P. J. (1994) *J. Opt. Soc. Am. A*, 11, 1491-1499. [6] Richard D. T. et al. (2011) *Planet. & Space Sci.*, 59, 1804-1814. [7] Hapke B. (2012) *Theory of Reflectance and Emittance Spectroscopy*, 2nd Ed.